CARBON 50 (2012) 2235–2243

Available at www.sciencedirect.com

SciVerse ScienceDirect

journal homepage: www.elsevier.com/locate/carbon

# Synthesis of sulfonated graphene/polyaniline composites with improved electroactivity

Elçin Coşkun [a,b], Erasto A. Zaragoza-Contreras [b], Horacio J. Salavagione [a,*]

[a] Instituto de Ciencia y Tecnología de Polímeros, CSIC, c/Juan de la Cierva, 3, 28006 Madrid, Spain
[b] Centro de Investigación en Materiales Avanzados (CIMAV), Av. Miguel de Cervantes, 120, 31109 Chihuahua, Mexico

ARTICLE INFO

*Article history:*
Received 28 October 2011
Accepted 12 January 2012
Available online 21 January 2012

ABSTRACT

The sulfonation of graphene by coupling with the diazonium salts of sulfanilic (SA) acid and amino-4-hydroxy-2-naphthalenesulfonic (NSA) acid is studied. Coupling with the diazonium salt of NSA gives the highest degree of sulfonation. Composites of polyaniline (PANI) and sulfonated graphene (SG) are prepared by the polymerization of aniline in the presence of the SG. The materials have been characterized by Raman, Fourier transformed infrared spectroscopy, thermogravimetric analysis and cyclic voltammetry. These materials are electrochemically active at pHs close to physiological pH due to the doping of PANI with the sulfonic groups in SG trapped in the polymer. Furthermore, good conductivity values are obtained.



## 1. Introduction

The outstanding properties of graphene, such as higher electron mobility [1], large specific surface area [2] and mechanical strength [3] have catapulted it to be one of the most studied and promising materials.

On the other hand, polyaniline (PANI) is the most investigated conducting polymer due to its facile synthesis, environmental stability, good electrical conductivity and uncommon conducting/insulating fast transition by doping/dedoping process [4]. This features have been exploited for use PANI in sensors [5–7], and more interestingly, in biosensors [8]. However, the electroactivity of pristine PANI strongly depends on the pH, being null at the pH required for bioassays due to undoping. To overcome that, the incorporation of an external dopant [9,10] as well as self-doping of PANI [11–13] have been the preferred approaches. However, the use of non-conductive external dopants, e.g. camphorsulfonic acid or poly(styrene sulfonate), and the breaking of ring-coplanarity, caused by the direct sulfonation of PANI, which improve the electroactivity, usually reduce the conductivity. For that reason the use of conductive materials as dopant would be interesting, and graphene emerges as a good candidate. Thus, graphene/PANI composites materials would merge the advantages of graphene (high electron mobility, i.e. fast signal transduction) and PANI (selectivity, specific chemistry, conductivity and electrochemical reversibility), meeting most of the conditions to be used as sensors. In fact it has been recently demonstrated that reduced graphene oxide acts as a counterion of PANI [14].

Despite composites of PANI with other carbon particles, i.e. carbon nanotubes (CNTs) [15–17] and carbon nanopipe/graphite nanosheets [18] have been explored, graphene brings together a number of advantages that make it better than other carbon particles, such as high aspect ratio, extraordinary electron mobility and low cost of production by oxidation/reduction of graphite, a natural allotrope of carbon.

Among the variety of methods of production of graphene-based polymer nanocomposites [19–22], graphene/PANI materials have been prepared principally by polymerization of aniline in the presence of graphene or its derivatives [23–26], being other approaches such as phase-transfer polymerization

* *Corresponding author:* Fax: +34 915644853.
E-mail address: horacio@ictp.csic.es (H.J. Salavagione).
0008-6223/$ - see front matter 
doi:10.1016/j.carbon.2012.01.041

[27] and mixing of preformed PANI with graphene [28] less explored. However, most of these studies are focused in the utilization of these composites as capacitors [23–25,28], while its ability for other applications has not been studied yet.

In this paper we report the controlled sulfonation of graphene with the final objective of using it to dope PANI for sensor applications. The doping of PANI with graphene's cousin, CNTs has been addressed using both carboxylated [16,29] and sulphonated CNTs [30–32]. In the case of graphene, the analog to carboxylated CNTs is graphite oxide (GO), carrying a large amount of defects in the $sp^2$ lattice that make it an insulator unless it is appropriately reduced.

In this work, the GO is reduced and subsequently sulfonated, and aniline polymerized in the presence of the sulfonated graphene (SG). The SG acts as a template for growing PANI and as the dopant of PANI, similarly to sulfonated CNTs [32] and sulfonated fullerene [33]. The SG/PANI composites show electroactivity at physiological pH which makes it, in principle suitable for application in biosensors. This improved electroactivity has not been observed in this study for GO/PANI materials.

## 2. Experimental

Graphite powder (45 μm), was purchased from Aldrich. The employed graphite oxide (GO) was synthesized by exhaustive oxidation of graphite powder accordingly to the Hummers method [34].

Aniline (Aldrich; p.a.) was distilled prior to use and stored at a low temperature. Sulfanilic acid (Aldrich, 99%), amino-4-hydroxy-2-naphthalenesulfonic acid (Fluka) and isopentyl nitrite (Aldrich) were used as received.

Potassium dihydrogen phosphate ($KH_2PO_4$), acetic acid ($CH_3COOH$) and sodium acetate ($CH_3COONa$) from Aldrich were employed to prepare buffers solutions.

### 2.1. Preparation of sulfonated graphene (SG)

GO (1 g) was dispersed in 250 mL of ultrapure water in a round-bottomed flask and was sonicated for 30 min. Then, 5 mL of 50% hydrazine solution was loaded and heated to 90 °C for 3 h. The material was filtered and washed repeatedly with water. The solid was dissolved in 250 mL of buffered solution at pH 8 to avoid precipitation [35] and 5.04 g (0.03 mol) of sulfanilic acid (SA) and 3 mL of isopentyl nitrite were subsequently added. The reaction flask was kept at 80 °C under magnetic stirring overnight. After cooling at room temperature, the product, called as GSA was filtered and washed with abundant water. The procedure was repeated for the sulfonation with amino-4-hydroxy-2-naphthalenesulfonic acid (NSA, 6.97 g; 0.03 mol) and the product was called as GNSA.

### 2.2. Synthesis of sulfonated graphene/PANI

The composites were prepared by polymerization of aniline in a solution containing dispersed SG. Briefly, 0.1 g of GSA was dispersed in 100 mL of water and treated with ultrasound for 20 min and 9 mL of HCl and 9.3 mL of aniline were then added. The dispersion was cooled to 0–5 °C in an ice bath and the oxidant (ammonium peroxydisulfate, $(NH_2)_4S_2O_8$, 5.7 g) was added to start polymerization. The polymerization was left to occur under vigorous stirring at 0 °C for 3 h. The product, called as GSA/PANI was filtered and washed with water, fallowed by drying under vacuum. The same procedure was employed for the preparation of PANI and GNSA and the material was called as GNSA/PANI.

### 2.3. Synthesis of graphite oxide/PANI

For comparison purposes, a composite of graphite oxide (GO) and PANI was prepared according to the procedure described above for SG/PANI.

### 2.4. Characterization

Fourier transform infrared spectroscopy (FTIR) spectra were collected in a Perkin Elmer Spectrum One spectrometer in transmission mode at a resolution of 4 $cm^{-1}$.

Raman measurements were undertaken in the Raman Microspectroscopy Laboratory of the Characterization Service in the Institute of Polymer Science and Technology, CSIC. A Renishaw InVia Reflex Raman system (Renishaw plc, Wotton-under-Edge, UK) was used, employing a grating spectrometer with a Peltier-cooled charge-coupled device detector coupled to a confocal microscope. All spectra were processed using Renishaw WiRE 3.2 software. The Raman scattering was excited using an Argon ion laser wavelength of 514.5 nm. The laser beam was focused on the sample with a 100× microscope objective (NA = 0.85), with a laser power at the sample of <2 mW.

Elemental composition was performed using a LECO CHNS-932 instrument.

TGA of powder materials was performed with a TA Instruments TQ-50, using nitrogen atmosphere at heating rate 10 °C $min^{-1}$ from ambient temperature to 900 °C.

The electrochemical measurements were conducted using screen printed electrodes in a DropSense cyclic voltammeter potentiostat. For sample preparation, 0.01 g of samples was dispersed in 5 mL of *N*-methyl-2-pyrrolidone (NMP). Then, 2 μL of each solution were drop-casted onto the carbon working electrode and dry under vacuum.

The electrolyte employed were HCl and buffered solutions of pH 2, 3, 5, 6 and 7. In the buffered solutions, 1 M of NaCl was added to maintain the ionic strength constant.

DC-conductivity measurements were carried out using the four-probe method on rigorously dry pellets. The measurements were carried out using a four-probe setup equipped with a dc current source (LCS-02) and a digital micro-voltmeter (DMV-001) from Scientific Equipment and Services. Prior to conductivity measurements, the polymers were redopped by 100 mL of 0.1 M HCl under magnetic stirring.

## 3. Results and discussion

Graphene was sulfonated by coupling with the diazonium salts of SA and NSA giving products that are soluble in water.

Although this procedure is somewhat different from other approaches involving a pre-reduction step [36,37], it is also successful. (Scheme S1). In both cases, the reactions succeeded as proved by FTIR, Raman, elementary analysis and TGA. However, the quantification by elementary analysis indicates that the yield of coupling is higher for GNSA; the ratio sulfonic groups/carbon atoms ($SO_3$/C) are 1/85 for GNSA and 1/120 for GSA. The reasons to explain that are not straightforward, but may be related to the life-time of the radicals formed.

In order to check whether the different sulfonation degree translate in different solubility we carried out UV–visible experiments in water. Using the experimental absorption coefficient for graphene dispersion in surfactant solutions (1390 L $g^{-1}$ $m^{-1}$) reported by Lotya et al. [38] we calculated the concentration of the dispersed material to be approximately 0.138 and 0.104 mg $mL^{-1}$ for GNSA and GSA, respectively.

The FTIR of GNSA shows bands corresponding to the symmetric (1095 $cm^{-1}$) and antisymmetric (1037 $cm^{-1}$) stretching of sulfonic groups in the modifying NSA (Fig. S1). Furthermore, bands at 1554 $cm^{-1}$ (C=C stretching of aromatic ring), 1384 $cm^{-1}$ (C—H stretching), 1259 $cm^{-1}$, 1162 $cm^{-1}$ (C—H in plane bending of aromatics) and 803 $cm^{-1}$ (C—H out of plane bending) also appear, confirming the success of the reactions (Fig. S1).

Raman spectra of the sulfonated materials clearly show the G ($sp^2$ carbon network) and D (defects in the $sp^2$ lattice) modes, and the higher order 2D and G + D modes (GO is shown for comparison). If we look at the D/G intensity ratio we see that it is higher for both sulfonated materials (GNSA = 0.92, NSA = 0.96) than that for GO (0.87) as was reported for covalently functionalized graphene [39,40]. The increase in the D/G ratio after reduction-functionalization has been attributed to the formation of smaller graphitic domains than those in the initial GO [41].

In the case of GO, the D and G bands appear at 1352 $cm^{-1}$ and 1598 $cm^{-1}$, respectively. However, for GSA and GNSA while the peak position of the D mode is also around 1353 $cm^{-1}$, that of the G mode appears shifted to around 1589 $cm^{-1}$ (GSA) and 1575 $cm^{-1}$ (GNSA), toward the value for graphite. This is due to the high number of defects, which makes that this broad band is conditioned by the overlap of the G and D′ mode [42], the latter related to edge defects. The deconvolution of this band allows us to compare the relative contribution of the D′ mode in the higher frequency band (Fig. 1). Clearly the contribution of this D′ band is higher in GO than in both SG, confirming improved order in the reduced-functionalized graphene sheets.

Finally, despite the high Raman efficiency of the D and G modes, a new peak is observed at 710 $cm^{-1}$, which can be attributed to C—S stretching.

Both sulfonated materials have better thermal stability than the starting GO, which clearly decompose around 200 °C due to pyrolysis of the labile oxygen-containing functional groups (Fig. S2) [42]. Clearly, the stability is due to the pre-reduction step removing these oxygen-containing functional groups. The stability is somewhat lower than that for reduced graphene oxide without further functionalization, which also proves the presence of some modifying groups

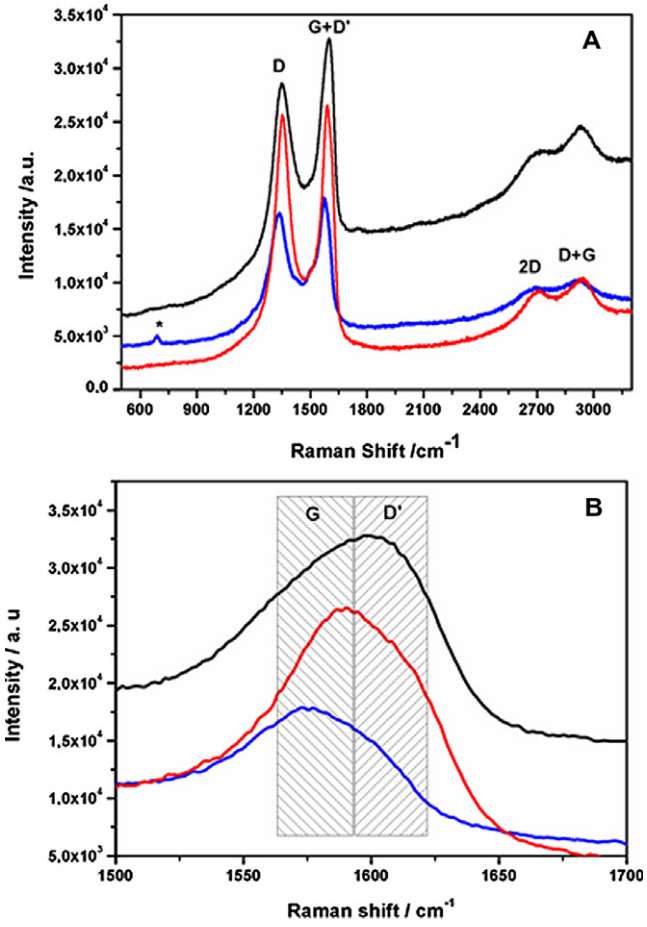


**Fig. 1 – Raman spectra of GO (black curves), GSA (red) and GNSA (blue). (B) Enlarged view of the region of the band composed by G and D′ modes. (For interpretation of the references to color in this figure legend, the reader is referred to the web version of this article.)**

bonded to the graphene sheets. In addition, the weight remaining after heating the sulfonated materials at 800 °C (70–72 wt.%) is similar to the obtained for covalently functionalized graphene nanoribbons obtained with the same synthetic procedure (reduction/diazonium coupling) [43].

Composites of both sulfonated materials were prepared as detailed in the experimental section. The FTIR spectra of the composites (GSA/PANI and GNSA/PANI) present the typical bands of PANI at 1560 $cm^{-1}$ (C=N, quinoid ring (Q) stretching), 1480 $cm^{-1}$ (C—C benzenoid ring (B) stretching), 1292 $cm^{-1}$ (C—N stretching of secondary amine), 1235 $cm^{-1}$ (C—N in BBB units), 1115 $cm^{-1}$ (C—H in plane bending of aromatic rings), 817 $cm^{-1}$ (C—H deformation in Q ring), and 796 $cm^{-1}$ (C—H out of plane bending of aromatic rings) (Fig. S3). It is remarkable the presence of two new bands in the sulfonated compounds, located at 1372 $cm^{-1}$ and 1260 $cm^{-1}$ (Fig. S3). While the first has already been observed in PANI and is assigned to C—N stretching in QBQ units [44], the second has been observed in doped PANI [45], suggesting that some internal doping of PANI by SG takes places. This is in agreement with a previous study on the doping of PANI with reduced graphene oxide, where the formation of a solid state charge

transfer complex has been proposed [14]. This effect can be confirmed analyzing the changes in the oxidation state of the polymer, where some differences between PANI obtained by the typical procedure and that polymerized in presence of sulfonated graphene can be observed. The Q/B intensity ratio ($I_{1560}/I_{1480}$) is ca. 10–15% lower for PANI than for PANI/GSA and PANI/GNSA, suggesting the presence of higher concentration of reduced segments in the composites as occurred for single-walled carbon nanotubes/PANI composites [16]. In that case the effect was attributed to $\pi$–$\pi$ interactions between CNTs and the PANI, where the oxidized CNTs reduce the PANI by charge transfer and the electron-donating ability of their carboxyl groups [16]. A similar explanation can be given in our system.

Finally, a shoulder can also be observed at 1034 $cm^{-1}$, which is attributable to the symmetric $SO_3$ stretching in the SG counterion.

The UV–visible spectra of GSA/PANI and GNSA/PANI resemble that of PANI (Fig. 2). The spectra in NMP show two bands at 330–334 nm (attributed to $\pi$–$\pi^*$ transition) and 632–635 nm, (assigned to the transition of the exciton of the quinone and related to the hopping electronic intra and interchain [46]). The first signal appears at a smaller wavelength than in PANI [46] probably due to a steric effect caused by the huge graphitic laminates that makes the transition energy increases. Furthermore, it is noted that the polaronic band shifts to lower energy in the case of both sulfonated materials. As the $\lambda_{max}$ of this band depends on the polymer oxidation [46,47], the shift can be produced by some doping of PANI with GSA and GNSA.

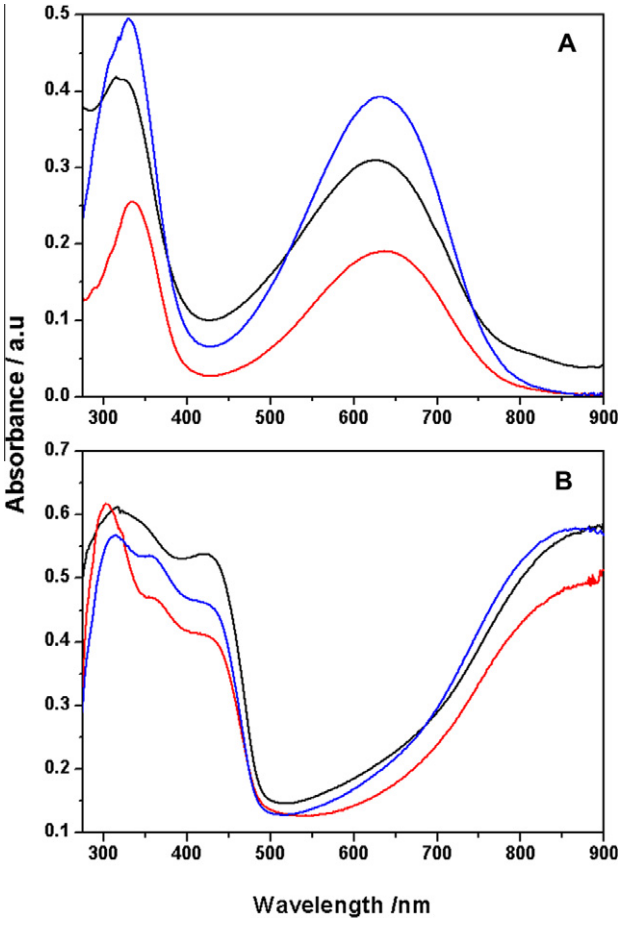


**Fig. 2 – UV–visible spectra of PANI (black line), GSA/PANI (red) and GNSA/PANI (blue) in NMP (A) and acidified with concentrated HCl (B). Concentration is 0.1 mg $mL^{-1}$ in all cases. (For interpretation of the references to color in this figure legend, the reader is referred to the web version of this article.)**

After acidifying the quartz cuvettes, the spectra show a new polaronic band at 420 nm while the initial polaronic band moves to larger wavelengths (800–900 nm) due to the external protonation. However, in this case the $\lambda_{max}$ appears at higher energies for both GSA/PANI and GNSA/PANI. This has also been observed in PANI doped with GO, and explained by a slight deprotonation of the polymer due to dissociation of carboxylic groups [14].

Thin films of both composites were prepared on the working electrode of screen-printed electrodes, allowing us to produce modified electrodes and to study the electroactivity of these materials (Fig. 3). The cyclic voltammograms of both GSA/PANI and GNSA/PANI in 1 M HCl electrolyte show a similar behavior to that of modified polyanilines [48] (Fig. 3). The oxidation peak, corresponding to the transition between the leucoemeraldine and emeraldine state of the polymer, slightly shifts to higher potentials in the sulfonated materials with respect to the pristine PANI. Probably, the sulfonic groups in graphene withdraw electrons from the aromatic ring, making the amine units more difficult to oxidize. In other words, this effect can also be related to the doping of PANI with the sulfonated graphene as was observed for composites of sulfonated CNTs and PANI [30].

In order to check the ability of GSA/PANI and GNSA/PANI-modified electrodes as sensors in different environments, including physiological pH, we conducted cyclic voltammetry in electrolytes with different pH values. As can be seen from Fig. 4, both composites show improved electroactivity, remaining electroactive at pHs close to physiological pH. In fact, a good electrochemical response is obtained at pH 6. Differently to self-doped PANI where the sulfonate groups take part of the polymer chain, here the SG sheets are trapped into the polymer. Probably the occluded SG protonates/dopes the PANI films changing the internal pH.

Similarly to self-doped sulfonated polyaniline [13] both peaks, corresponding to the leucoemeraldine/emeraldine and emeraldine/pernigraniline states of PANI, tend to overlap at an intermediate potential with increasing pH. That means that the transition leucoemeraldine/emeraldine is more difficult, while the transition emeraldine/pernigraniline is easier, as the pH increases. However in the case of GSA/PANI and GNSA/PANI, after overlapping, the new peak moves to lower potentials as the pH increases, following the tendency of the second peak (Figs. 4 and 5). In other words, the second transition varies similarly to PANI; but the first transition potential increases at lower pHs (similar to sulfonated PANI [13]) and then decreases as the pH increases (in the case of PANI this process in independent of the pH, and only anion insertion occurs [49,50]) (Fig. 5).

The reason why this happens is uncertain and could be related to (i) a change in the ion exchange mechanism of the first process, i.e. the polymer releases protons during

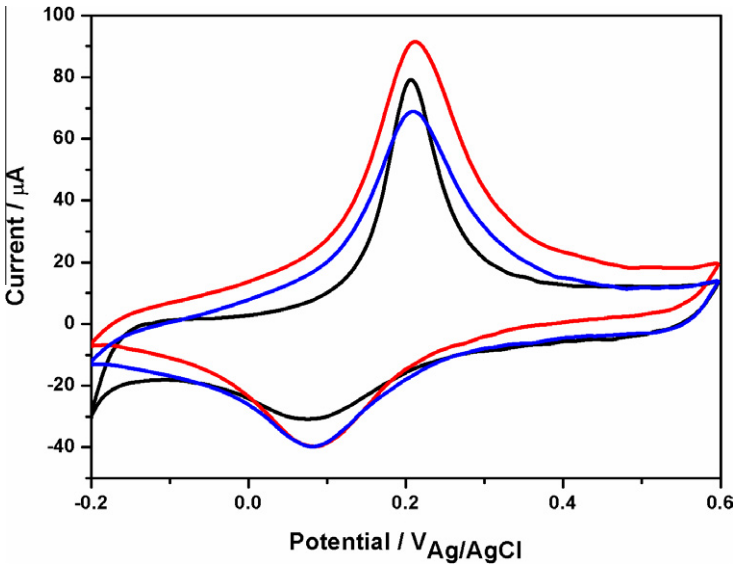


**Fig. 3 – Cyclic voltammograms of PANI (black line), GSA/PANI (red) and GNSA/PANI (blue)-modified GC electrodes in HCl 1 M. Scan rate = 50 mV $s^{-1}$. (For interpretation of the references to color in this figure legend, the reader is referred to the web version of this article.)**

oxidation up to a certain value of pH, and over this pH it start to uptake protons or (ii) the disappearance of one of the intermediate states of oxidation of PANI.

Although the ionic exchange of the first process for GSA/PANI and GNSA/PANI is hard to estimate, the second is relatively easy with the Nernst equation for the system, which allows us estimating the number of electrons and protons entering/leaving the polymer film to neutralize the charge generated (see supporting information for details on how to obtain the equation).

$$E_p = E_f - 0.059\frac{n_H}{n_e}pH$$

The slopes of GSA/PANI (134 mV·$pH^{-1}$) and GNSA/PANI (137 mV·$pH^{-1}$) are similar to that of PANI (118 mV·$pH^{-1}$) and four times greater than that of sulfonated PANI (37 mV·$pH^{-1}$) (Fig. 5). This means that GSA/PANI and GNSA/PANI expels 4 protons and uptakes 2 electrons (equal to PANI [50]), while for sulfonated PANI it expels only 1 proton per 2 electrons. However, these results should be confirmed by quartz crystal microbalance and probe beam deflection measurements [51], while the presence of the intermediate state should be proved by in situ spectroscopies, such as FTIR, Raman or EPR.

In the best of our knowledge, studies on the pH-dependence of the electrochemistry of similar systems, i.e. sulfonated CNTs/PANI composites have not been reported. However, nanocomposites prepared by layer-by-layer assembly of poly(sodium 4-styrenesulphonate) (PSS) wrapped CNTs with polyaniline nanofibers have shown good

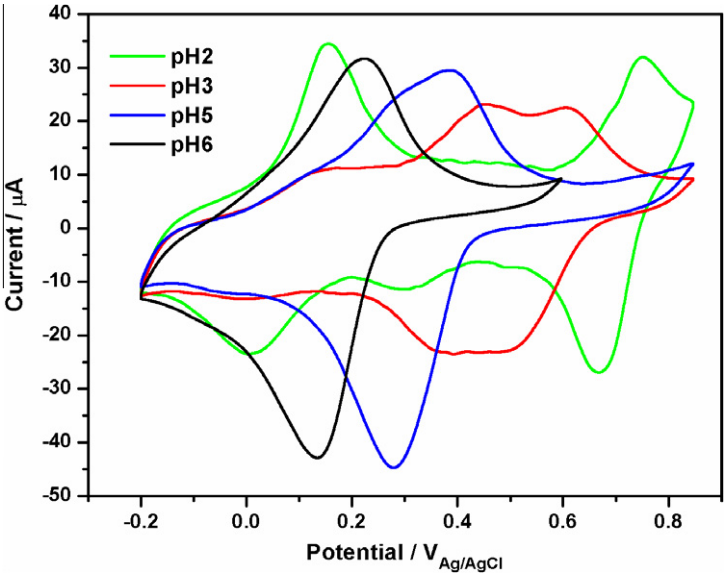


**Fig. 4 – Cyclic voltammograms of GNSA/PANI at different pH electrolytes. Scan rate 50 mV $s^{-1}$.**

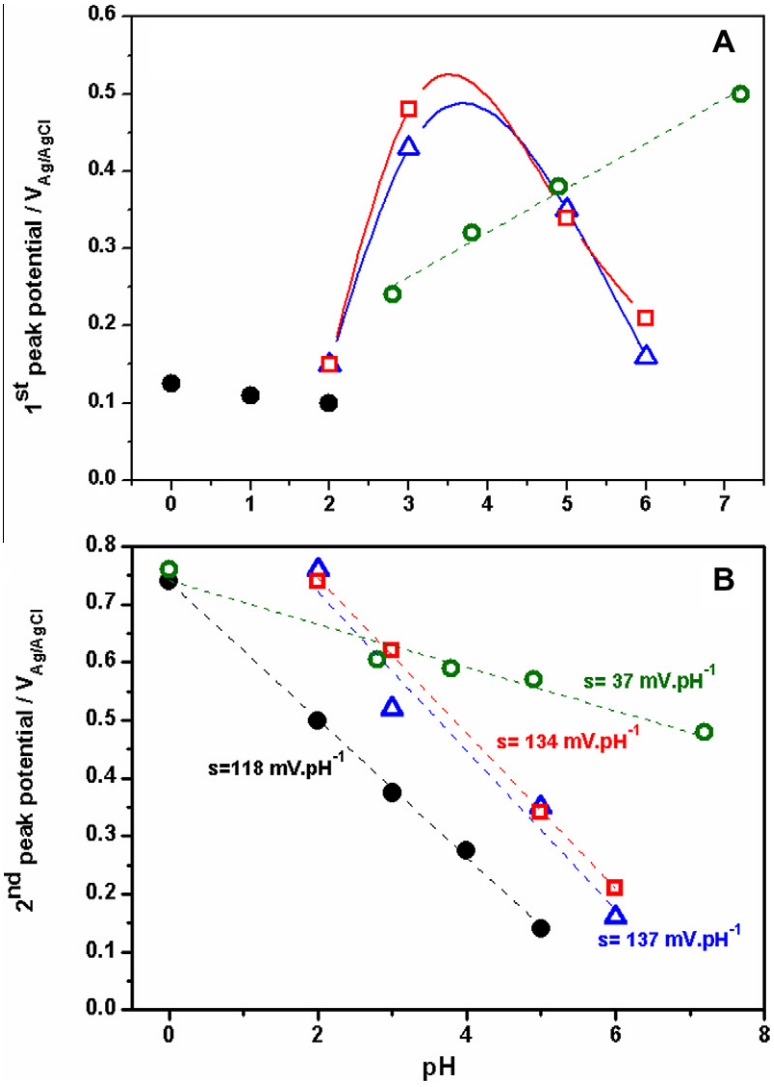


**Fig. 5 – Variation of the first (A) and second (B) peak potential with the electrolyte pH for GSA/PANI (red) and GNSA/PANI (blue). Data of PANI (black) and sulfonated PANI (green) are also shown for comparison. The slopes obtained by linear fit with the Nernst equation for the second process is shown in (B). (For interpretation of the references to color in this figure legend, the reader is referred to the web version of this article.)**

electrochemical response at neutral (or even basic) pH [52]. But, in this case, the first redox process shows a linear pH-dependence with a slope value very close to that for PANI. Differences between the PSS/CNTs/PANI composite and our systems seem logical since in the former the PANI is assembled by electrostatic interactions with the PSS surrounding the CNTs, while in our approach PANI growth on the graphene surface allowing a more intimate contact.

On the other hand, considering the high density of surface carboxylate groups in GO, a potential doping of PANI with GO should extend the electroactivity of PANI at higher pH values. However, the electrochemical behavior of GO/PANI composites is quite different from that for PANI/GSA and PANI/GNSA (Fig. S5). In this case, the cyclic voltammograms became more resistive as the pH increased and the redox peaks were difficult to distinguish at values over 4, probably due to the insulating character of GO.

Finally, taking profit of the electroactivity at higher pH we carried out a series of preliminary experiments to detect ferrocenium ($Fc^+$) at pH 6 (Fig. 6) [53]. Although the GNSA/PANI-modified GC electrode shows some signal due to the polymer, it can be noted that the peak potential of $Fc/Fc^+$ redox couple does not change for GNSA/PANI-modified GC electrode with respect to the bare GC.

As one of the main challenges in these systems is to extend the electroactivity without loosing electrical conductivity, we analyzed it using the four-probe method. Contrary to what happens with self-doped PANI, in our case the materials exhibit higher electrical conductivity than the pristine PANI. The DC-conductivity values were 1.42, 25.6 and 26.3 S $cm^{-1}$ for pristine PANI, GSA/PANI and GNSA/PANI, respectively. The improvements in conductivity in SG-doped PANI can be due to the graphene sheets acts as a bridge for the electronic hopping between PANI chains.

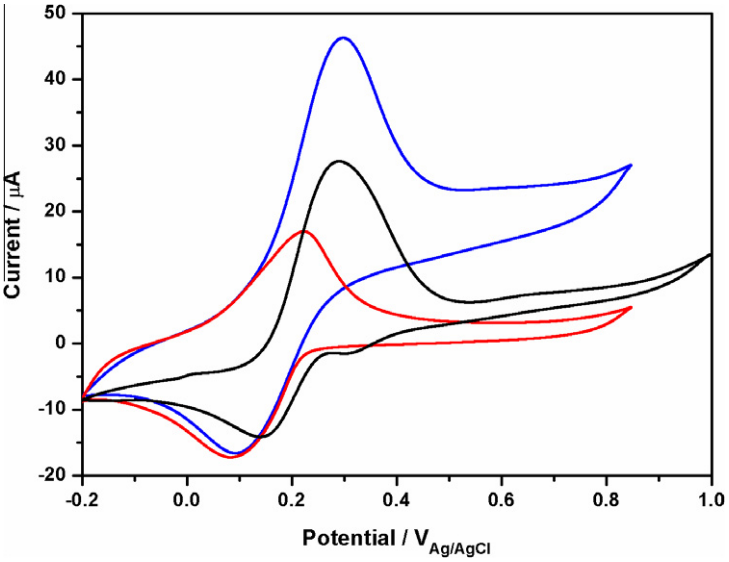


**Fig. 6 – Cyclic voltammograms of bare (black curve) and GNSA/PANI-modified (blue) GC electrodes in phosphate buffers (pH 6) + 1 mM ferricinium solution. The response of GNSA/PANI in absence of ferrocenium (red) is also shown for comparison. Scan rate 50 mV $s^{-1}$. (For interpretation of the references to color in this figure legend, the reader is referred to the web version of this article.)**

In fact, GO/PANI gives the lowest conductivity value (1.1 S $cm^{-1}$) due to the presence of insulating GO between PANI chains, as expected.

## 4. Conclusions

Composites of PANI and graphene derivatives have been prepared by in situ polymerization of aniline in the presence of SG. The SG, which acts as external dopant of PANI, has a main advantages respect to other sulfonated dopants or sulfonated PANI: it is intrinsically conductive. In fact, sulfonated graphene/PANI demonstrated 20 times higher electrical conductivity than pure PANI.

Furthermore, the SG occluded into the polymer produces some change the internal pH of polymer films making it electroactive at higher pH electrolytes than PANI. The ionic exchange of PANI/sulfonated graphene composites is somewhat different from that of PANI and sulfonated PANI, especially in the first redox process. The ionic exchange is open for future studies, especially in situ experiment that can help to understand the redox processes.

## Acknowledgments

Financial support from MICINN (Project: MAT2009-09335) is gratefully acknowledged. E.C. thanks CONACYT Mexico for a graduate fellowship. H.J.S. thanks MICINN for a Ramón y Cajal Postdoctoral Fellowship.

## Appendix A. Supplementary data

Supplementary data associated with this article can be found, in the online version, at doi:10.1016/j.carbon.2012.01.041.

## REFERENCES

[1] Geim AK, Novoselov KS. The rise of graphene. Nat Mater 2007;6(3):183–91.
[2] Stoller MD, Park S, Zhu Y, An J, Ruoff RS. Graphene-based ultracapacitors. Nano Lett 2008;8(10):3498–502.
[3] Lee C, Wei X, Kysar LW, Hone J. Measurement of the elastic properties and intrinsic strength of monolayer graphene. Science 2008;321(5887):385–8.
[4] Bhadra S, Khastgira D, Singha NK, Lee JH. Progress in preparation, processing and applications of polyaniline. Prog Polym Sci 2009;34(8):783–810.
[5] Virji S, Huang J, Kaner RB, Weiller BH. Polyaniline nanofiber gas sensors: examination of response mechanisms. Nano Lett 2004;4(3):491–6.
[6] Wang J, Chan S, Carlson RR, Luo Y, Ge G, Ries RS, et al. Electrochemically fabricated polyaniline nanoframework electrode junctions that function as resistive sensors. Nano Lett 2004;4(9):1693–7.
[7] Zhu S, Gu J, Chen Z, Dong J, Liu X, Chen C, et al. Controlled synthesis of polyaniline inside mesoporous carbon for electroanalytical sensors. J Mater Chem 2010;20(24):5123–8.
[8] Dhand C, Das M, Datta M, Malhotra BD. Recent advances in polyaniline based biosensors. Biosens Bioelect 2011;26(6):2811–21.
[9] Lukachova LV, Shkerin EA, Puganova EA, Karyakina EE, Kiseleva SG, et al. Electroactivity of chemically synthesized polyaniline in neutral and alkaline aqueous solutions: role of self-doping and external doping. J Electroanal Chem 2003;544:59–63.
[10] Tian SJ, Baba A, Liu JY, Wang ZH, Knoll W, Park MK, et al. Electroactivity of polyaniline multilayer films in neutral solution and their electrocatalyzed oxidation of β-nicotinamide adenine dinucleotide. Adv Funct Mater 2003;13(6):473–9.
[11] Yue J, Epstein AJ. Electronic control of pH at sulfonated polyaniline electrodes. J Chem Soc Chem Commun 1992;21:1540–2.

[12] Salavagione H, Morales GM, Miras MC, Barbero B. Synthesis of a self-doped polyaniline by nucleophilic addition. Acta Polym 1999;50(1):40–4.
[13] Sanchís Bermúdez C, Salavagione HJ, Arias Pardilla J, Morallón E. Tuning the electroactivity of conductive polymer at physiological pH. Electrochim Acta 2007;52(9):2978–86.
[14] Vallés C, Jiménez P, Muñoz E, Benito AM, Maser WK. Simultaneous reduction of graphene oxide and polyaniline: doping-assisted formation of a solid-state charge-transfer complex. J Phys Chem C 2011;115(21):10468–74.
[15] Sainz R, Benito AM, Martínez MT, Galindo JF, Sotres J, Baró AM, et al. Soluble self-aligned carbon nanotube/polyaniline composites. Adv Mater 2005;17(3):278–81.
[16] Liao Y, Zhang C, Zhang Y, Strong V, Tang J, Li X-G, et al. Carbon nanotube/polyaniline composite nanofibers: facile synthesis and chemosensors. Nano Lett 2011;11(3):954.
[17] Lafuente E, Callejas MA, Sainz R, Benito AM, Maser WK, Sanjuán ML, et al. The influence of single-walled carbon nanotube functionalization on the electronic properties of their polyaniline composites. Carbon 2008;46:1909–17.
[18] Venkata Ramana G, Padya B, Srikanth VVSS, Jain PK, Padmanabham G, Sundararajan G. Electrically conductive carbon nanopipe–graphite nanosheet/polyaniline composites. Carbon 2001;49(15):5239–45.
[19] Choi E-Y, Han TH, Hong J, Kim JE, Lee SH, Kim HW, et al. Noncovalent functionalization of graphene with end-functional polymers. J Mater Chem 2010;20(10):1907–12.
[20] Lee SH, Kim HW, Hwang OJ, Lee WJ, Kwon J, Bielawski CW, et al. Three-dimensional self-assembly of graphene oxide platelets into mechanically flexible macroporous carbon films. Angew Chem Int Ed 2010;49(52):10084–8.
[21] Pots JR, Dreyer DR, Bielawski CW, Ruoff RS. Graphene-based polymer nanocomposites. Polymer 2011;52(1):5–25.
[22] Salavagione HJ, Martínez G, Ellis G. Recent advances in the covalent modification of graphene with polymers. Macromol Rapid Commun 2011;32(22):1771–89.
[23] Wang H, Hao Q, Yang X, Lu L, Wang W. A nanostructured graphene/polyaniline hybrid material for supercapacitors. Nanoscale 2010;2(10):2164–70.
[24] Zhang K, Zhang LL, Zhao XS, Wu J. Graphene/polyaniline nanofiber composites as supercapacitor electrodes. Chem Mater 2010;22(4):1392–401.
[25] Wang DW, Li F, Zhao J, Ren W, Chen ZG, Tan J, et al. Fabrication of graphene/polyaniline composite paper *via in situ* anodic electropolymerization for high-performance flexible electrode. ACS Nano 2009;3(7):1745–52.
[26] Goswami S, Maiti UN, Maiti S, Nandy S, Mitra MK, Chattopadhyay KK. Preparation of graphene–polyaniline composites by simple chemical procedure and its improved field emission properties. Carbon 2011;49(7):2245–52.
[27] Hao Q, Wang H, Yang Z, Lu L, Wang X. Morphology-controlled fabrication of sulfonated graphene/polyaniline nanocomposites by liquid/liquid interfacial polymerization and investigation of their electrochemical properties. Nano Res 2011;4(4):323–33.
[28] Wu Q, Xu Y, Yao Z, Liu A, Shi G. Supercapacitors based on flexible graphene/polyaniline nanofiber composite films. ACS Nano 2010;4(4):1963–70.
[29] Choudhury A, Kar P. Doping effect of carboxylic acid group functionalized multi-walled carbon nanotube on polyaniline. Composites: Part B 2011;42(6):1641–7.
[30] Zhu Z-Z, Wang G-C, Sun M-Q, Li X-W, Li C-Z. Fabrication and electrochemical characterization of polyaniline nanorods modified with sulfonated carbon nanotubes for supercapacitor applications. Electrochim Acta 2011;56(3):1366–72.
[31] Ding M, Tang Y, Gou P, Reber RJ, Star A. Chemical sensing with polyaniline coated single-walled carbon nanotubes. Adv Mater 2011;23(4):536–40.
[32] Wei Z, Wan M, Lin T, Dai L. Polyaniline nanotubes doped with sulfonated carbon nanotubes made via a self-assembly process. Adv Mater 2003;15(2):136–9.
[33] Qiu H, Wan M, Matthews B, Dai L. Conducting polyaniline nanotubes by template-free polymerization. Macromolecules 2001;34(4):675–7.
[34] Hummers WS, Offeman RE. Preparation of graphitic oxide. J Am Chem Soc 1958;80(6):1339.
[35] Li D, Müller MB, Gilje S, Kaner RB, Wallace GG. Processable aqueous dispersion of graphene nanosheets. Nat Nanotechnol 2008;3(2):101–5.
[36] Si Y, Samulski ET. Synthesis of water soluble graphene. Nano Lett 2008;8(6):1679–82.
[37] Zhao G, Jiang L, He Y, Li J, Dong H, Wang X, et al. Sulfonated graphene for persistent aromatic pollutant management. Adv Mater 2011;23(34):3959–63.
[38] Lotya M, Hernandez Y, King PJ, Smith RJ, Nicolosi V, Karlsson VLS, et al. Liquid phase production of graphene by exfoliation of graphite in surfactant/water solutions. J Am Chem Soc 2009;131(10):3611–20.
[39] Niyogi S, Bekyarova E, Itkis ME, Zhang H, Shepperd K, Hicks J, et al. Spectroscopy of covalently functionalized graphene. Nano Lett 2010;10(10):4061–6.
[40] Castelaín M, Martínez G, Merino P, Martín-Gago JA, Segura JL, Ellis G, et al. Graphene functionalization with a conjugated poly(fluorene) via "click" coupling. Striking electronic properties in solution. Chem. Eur. J. 2011. doi:10.1002/chem.201102008.
[41] Stankovich S, Dikin DA, Piner RD, Kohlhaas KA, Kleinhammes A, Jia Y, et al. Synthesis of graphene-based nanosheets via chemical reduction of exfoliated graphite oxide. Carbon 2007;45(7):1558–65.
[42] Cançado LG, Pimenta MA, Neves BRA, Dantas MSS, Jorio A. Influence of the atomic structure on the Raman spectra of graphite edges. Phys Rev Lett 2004;93(24):247401–4.
[43] Zhu Y, Higginbotham AL, Tour JM. Covalent functionalization of surfactant-wrapped graphene nanoribbons. Chem Mater 2009;21(21):5284–91.
[44] Trchová M, Stejskal J. The infrared spectroscopy of conducting polymer nanotubes. Pure Appl Chem 2011;83:1803–7.
[45] Boyer MI, Quillard S, Louarn G, Froyer G, Lefrant S. Vibrational study of the $FeCl_3$-doped dimer of polyaniline; a good model compound of emeraldine salt. J Phys Chem B 2000;104(38):8952–61.
[46] Stafstrom S, Bredas JL, Epstein AJ, Woo HS, Tanner DB, Huang WS, et al. Polaron lattice in highly conducting polyaniline: theoretical and optical studies. Phys Rev Lett 1987;59(13):1464–7.
[47] Masters JG, Sun Y, MacDiarmid AG. Epstein AJ Polyaniline: allowed oxidation states. Synth Met 1991;41(1–2):715–8.
[48] Barbero C, Salavagione HJ, Acevedo DF, Grumelli DE, Garay F, Planes GA. Novel synthetic methods to produce functionalized conducting polymers I. Polyanilines. Electrochim Acta 2007;49(22–23):3671–86.
[49] Barbero C, Miras MC, Haas O, Kötz R. Direct in situ evidence for proton anion-exchange in polyaniline films by means of probe beam deflection. J Electrochem Soc 1991;138(3):669–72.
[50] Huang WS, Humphrey BD, McDiarmid AG. Polyaniline, a novel conducting polymer. Morphology and chemistry of its oxidation and reduction in aqueous electrolytes. J Chem Soc, Faraday Trans 1986;82(8):2385–400.

[51] Salavagione HJ, Arias-Pardilla J, Pérez JM, Vázquez JL, Morallón E, Miras MC, et al. Study of redox mechanism of poly(o-aminophenol) using in situ techniques: evidence of two redox processes. J Electroanal Chem 2005;576(1):139–45.
[52] Hu Z, Xu J, Tian Y, Peng R, Xian Y, Ran Q, et al. Layer-by-layer assembly of poly(sodium 4-styrenesulfonate) wrapped multiwalled carbon nanotubes with polyaniline nanofibers and its electrochemistry. Carbon 2010;48(13):3729–36.
[53] Sanchis C, Salavagione HJ, Morallon E. Ferrocenium strong adsorption on sulfonated polyaniline modified electrodes. J Electroanal Chem 2008;618(1–2):67–73.